The Ornstein-Uhlenbeck Process Does Not Reproduce Spiking Statistics of Neurons in Prefrontal Cortex

Shigeru Shinomoto
Yutaka Sakai
Department of Physics, Graduate School of Science, Kyoto University, Sakyo-ku, Kyoto 606-8502, Japan

Shintaro Funahashi
Laboratory of Neurobiology, Faculty of Integrated Human Studies, Kyoto University, Sakyo-ku, Kyoto 606-8501, Japan

Cortical neurons of behaving animals generate irregular spike sequences. Recently, there has been a heated discussion about the origin of this irregularity. Softky and Koch (1993) pointed out the inability of standard single-neuron models to reproduce the irregularity of the observed spike sequences when the model parameters are chosen within a certain range that they consider to be plausible. Shadlen and Newsome (1994), on the other hand, demonstrated that a standard leaky integrate-and-fire model can reproduce the irregularity if the inhibition is balanced with the excitation. Motivated by this discussion, we attempted to determine whether the Ornstein-Uhlenbeck process, which is naturally derived from the leaky integration assumption, can in fact reproduce higher-order statistics of biological data. For this purpose, we consider actual neuronal spike sequences recorded from the monkey prefrontal cortex to calculate the higher-order statistics of the interspike intervals. Consistency of the data with the model is examined on the basis of the coefficient of variation and the skewness coefficient, which are, respectively, a measure of the spiking irregularity and a measure of the asymmetry of the interval distribution. It is found that the biological data are not consistent with the model if the model time constant assumes a value within a certain range believed to cover all reasonable values. This fact suggests that the leaky integrate-and-fire model with the assumption of uncorrelated inputs is not adequate to account for the spiking in at least some cortical neurons.

1 Introduction

There are a large number of single-neuron models designed to reproduce aspects of spiking statistics, such as the probability density of interspike intervals (ISIs). Although some models can reproduce the observed statistics, the physiological meaning of model parameters has not yet been thor-

oughly examined. For example, although Gerstein and Mandelbrot (1964) presented a successful fitting of the first passage time distribution function of the Wiener process to the real ISI histograms of a neuron in the cat cochlear nucleus, one cannot relate the parameters determined in this fitting with the concrete membrane dynamics of a biological neuron. Alternatively, one can assume an accumulated Poisson excitation process as the concrete spiking mechanism. By fitting the model ISI distribution with the real ISI histograms, however, it is found that, assuming this model, a neuron should generate a spike with only a few excitation inputs (see, for instance, Tuckwell, 1988). This runs counter to our basic knowledge of the neuronal spiking processes, outlined as follows.

A typical cortical neuron receives spiking signals from thousands of neurons (Ishizuka, private communication, 1998; Ishizuka, Cowan, & Amarel, 1995; Abeles, 1991). The number of spikes arriving within an interval of length equal to the membrane time constant is also large, and the fluctuation in the accumulated potential is expected to be relatively small. Thus, the membrane potential should increase regularly, and a neuron should generate temporally regular spikes. Cortical neurons, however, do not actually generate regular spike sequences, although motoneurons do. This is the point of the discussion by Softky and Koch (1993). They concluded that some strong nonlinearity is necessary in single-neuron models to reproduce the spiking irregularity.

In the discussion by Softky and Koch, it is assumed that the mean excitation is greater than the mean inhibition. If the inhibition is comparable to the excitation, however, the net input becomes small, and its fluctuation is relatively large. The balanced inhibition thus causes the cell to possess a membrane potential that behaves similarly to a random walk and a high irregularity of the spike sequence. Even the simple leaky integrate-and-fire model can reproduce the spiking irregularity. This is the point addressed by Shadlen and Newsome (1994).

The Ornstein-Uhlenbeck process, which is naturally derived from the leaky integration assumption, can in fact generate the irregular spike sequence by means of balanced inhibition. There are several studies concerning the manner in which balanced inhibition is brought about naturally in model networks (Tsodyks & Sejnowski, 1995; van Vreeswijk & Sompolinsky, 1996; Amit & Brunel, 1997). However, our knowledge of the physiological parameters of biological neurons is not yet sufficient to specify the parameter range of a single-neuron model. It is not easy to control the inhibition balance for a neuron whose spike rate is changing (Shinomoto & Sakai, 1998).

Thus, we wish to determine the suitability of the Ornstein-Uhlenbeck process by studying actual biological spiking data. In this way, we estimate not only the coefficient of variation (CV), which is a measure of the spiking irregularity, but also the skewness coefficient (SK), which is a measure of

the asymmetry of the ISI distribution. The consistency of the spiking data with the Ornstein-Uhlenbeck process will be examined using these two coefficients. If a biological spike sequence consists of a very large number of ISIs, then we can employ higher-order statistical coefficients in addition to these two for the examination of data, or we can construct a detailed ISI histogram for direct comparison with the model distribution function. However, the number of ISIs included in each of our biological data sets is on the order of 100, which is not large enough to justify the employment of additional coefficients.

There have been several studies in which biological data were examined on the basis of certain statistical coefficients. The statistical coefficients Lánský and Radil (1987) studied are not CV and SK, but SK and the coefficient of excess, the latter of which contains the fourth-order moment. In that study, a spike sequence is identified with a single point on the plane defined by these two statistical coefficients. Spiking data recorded from neurons in the cat mesencephalic reticular formation were found to be widely distributed on this plane, and these authors were not able to use their results to select a particular model process from several that are typically used, such as the Poisson process (which generates the exponential distribution of ISIs), the accumulated Poisson excitation process (the gamma distribution), and the Wiener process (the inverse-gauss distribution). Inoue and Sato (1993) performed numerical simulations of the Ornstein-Uhlenbeck process with a variety of parameter sets and also plotted their results on the plane determined by these two coefficients, SK and coefficient of excess. Inoue, Sato, and Ricciardi (1995) attempted to fit the ISI distribution of the Ornstein-Uhlenbeck process to ISI histograms taken from mesencephalic neurons. To our knowledge, however, the consistency of biological data with a single-neuron model has never been tested with statistical rigor.

If a spike sequence is generated by a specific single-neuron model, the model parameters, which specify intraneuronal conditions and the statistical characteristics of incoming inputs, determine the shape of ISI distribution and thus also the statistical coefficients, such as CV and SK. By sweeping through values of the model parameters, we can specify the region of feasible (CV, SK) values for a specific single-neuron model. If the statistical coefficients (CV, SK) obtained from biological data deviate significantly from the model-feasible region, taking into account possible deviation due to the finite number of ISIs, then the single-neuron model should be rejected. We will take up the spiking data recorded from the prefrontal cortex of rhesus monkeys while performing a delay-response task (Funahashi, Hara, & Inoue, 1999). By plotting the data and the feasible region of the Ornstein-Uhlenbeck process onto the CV-SK plane, we have found that they are inconsistent with each other.

2 The Biological Data

In this section, we briefly summarize the delay response experiment by Funahashi (1998), whose task paradigm is identical to one of the varieties in Funahashi, Bruce, and Goldman-Rakic (1989) and Goldman-Rakic, Bruce, and Funahashi (1990). We will also explain the methods we use in preparing data for analysis here.

A monkey is trained to fixate its eyes on a central spot that appears in a cathode ray tube. Eye position is monitored by a magnetic search coil. After the monkey has maintained fixation for 0.75 sec, a cue spot is presented for 0.5 sec at a position selected randomly from eight peripheral locations (see Figure 1a). The monkey is required to maintain fixation on the central spot when the cue spot appears in the peripheral region and throughout the subsequent delay period of 3 sec in which the cue stimulus is absent. After the delay period, which is signaled by the extinction of the fixation spot, the monkey is expected to make a saccadic eye movement within 0.5 sec. If the saccade falls within some diameter of the cue position, the monkey is rewarded with a drop of water or juice. After a training period of a few months, all monkeys became capable of performing the task with a success rate of 90% or more. In this study, we are interested in the spiking data of successful trials, and thus we ignore all unsuccessful trials.

Throughout the repetition of the delay-response task, the spiking of a neuron was recorded from the principal sulcus in the prefrontal cortex. The neuronal spike rate generally changes in response to changes in experimental conditions. Within the delay period, neurons appear to exhibit a sustained spike rate. In some neurons, the level of the sustained spike rate depends largely on the choice of cue stimuli (see Figure 1b). This suggests that the cue information (short-term memory) is preserved in the form of activity patterns of neuronal assembly in a region somewhere about the prefrontal cortex during the 3 sec delay period. It is interesting to note that the recorded spike sequences display a large CV value (~ 1), which is nearly independent of the mean spike rate. Shinomoto and Sakai (1998) pointed out the inability of the leaky integrate-and-fire model to preserve the spiking irregularity, but we do not address this problem here.

We considered only the middle 2 sec in the delay period of 3 sec in order to avoid the possible initial and final transient changes. The number of spikes contained in this 2 sec is typically fewer than 20, which is too small to obtain a reliable estimate of the statistical coefficients. In order to obtain a long spike sequence, we linked spike sequences of different trials with the same cue stimulus, assuming that for each trial corresponding to a given cue stimulus, each neuron is subject to the same conditions. If a linked spike sequence contains more than 100 spikes, we cut off a sequence of 100 ISIs to calculate the statistical coefficients CV and SK.

We tested two methods of linkage. In the first method (LINKAGE1, L1), we simply linked the 2 sec records to make up a long time series. In this
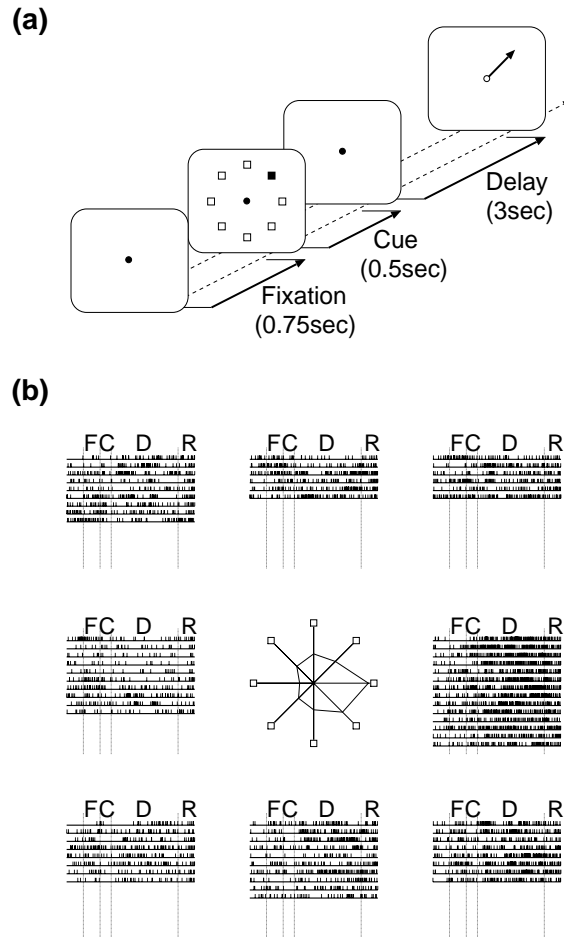
Figure 1: (a) Schematic representation of the delay-response task. (b) Spiking sequences of one principal sulcus neuron, classified according to the cue stimulus. F, C, D, and R represent the fixation period, cue period, delay period, and response period, respectively. The cue stimulus is chosen randomly from the eight directions, and for this reason the number of trials varies with direction. The plot in the center is the delay period spike rate (radial) as a function of cue position (angle).

method, the period of time τ_1 after the final spike in one 2 sec record and the period of time τ_2 before the first spike of the succeeding 2 sec record are combined to form a single interval of length $\tau_1 + \tau_2$. In another method (LINKAGE2, L2), we linked interspike intervals included in 2 sec records by ignoring the first and the last fragmentary intervals. In the latter method, any 2 sec record that contains fewer than two spikes is ignored entirely, and long intervals are removed. Thus, L2 has a tendency to shorten the mean spike interval, while L1 preserves it.

We examined spiking data recorded from 233 neurons. The total number of successful trials recorded with respect to each neuron was about 70. We divided the data according to the eight types of cue stimuli and made up $233 \times 8 = 1864$ linked spike sequences for each method of linkage. Among these 1864 linked spike sequences prepared by means of L1, 666 (35.7%) contained more than 100 spikes. Among these prepared using L2, 611 (32.8%) contained more than 100 spikes. Figure 2 summarizes the sets of 100 ISIs prepared with the above described methods in the plane defined by the statistical coefficients CV and SK, whose precise definitions are given in the succeeding section.

3 Statistical Coefficients of a Spike Sequence

Data are examined in this article on the basis of two dimensionless statistical coefficients: the coefficient of variation CV, and the skewness coefficient SK. The CV is a measure of variability of ISIs, defined as the ratio of the standard deviation to the mean,

$$\mathrm{CV} = \frac{\overline{(T - \overline{T})^2}^{1/2}}{\overline{T}},$$

where T is the interspike interval, and $\overline{\cdots}$ represents an averaging operation: $\overline{x} = \frac{1}{n} \sum_{i=1}^{n} x_i$. For the sake of producing an unbiased estimation of the mean squared deviation, we must revise $\overline{(T - \overline{T})^2}$ from $\frac{1}{n} \sum_{i=1}^{n} (T_i - \overline{T})^2$ to $\frac{1}{n-1} \sum_{i=1}^{n} (T_i - \overline{T})^2$.

The SK is a measure of the asymmetry of the interval distribution, defined as

$$\mathrm{SK} = \frac{\overline{(T - \overline{T})^3}}{\overline{(T - \overline{T})^2}^{3/2}}.$$

It should be stressed that any definite distribution function whose moments $\overline{T^\mu}$ are finite uniquely determines the coefficients CV and SK, but the two coefficients CV and SK alone do not uniquely determine the shape of a distribution.

It is easy to calculate $(\mathrm{CV}, \mathrm{SK})$ for a distribution function given in a closed form. For instance, a simple Poisson process in which spikes are
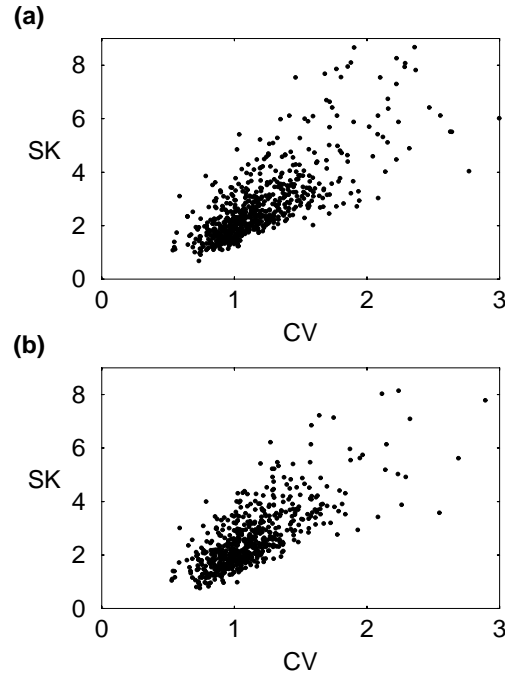
Figure 2: Dots represent the estimated (CV, SK) values of the spike sequences of 100 ISIs. Plots (a) and (b) respectively represent the data prepared according to the methods L1 and L2.

generated randomly in time with some fixed mean rate yields an exponential distribution of intervals,

$$p(T) = a \exp(-aT).$$

This exponential distribution gives $(CV, SK) = (1, 2)$.

In the accumulated Poisson excitation process, a neuron generates a spike when the number of incoming excitation inputs following the preceding spiking event reaches a certain fixed value. This accumulated Poisson excitation process leads to a gamma distribution,

$$p(T) = a^b T^{b-1} \exp(-aT)/\Gamma(b),$$

where b is the number of excitation inputs needed for a neuron to emit a spike, and $\Gamma(b)$ is the gamma function. For the gamma distribution, the points (CV, SK) lie on the line $SK = 2CV$.

In the Wiener process, the neuronal membrane potential is characterized by a one-dimensional random walk with a constant drift force. A neuron

generates a spike if the potential exceeds some threshold level, and then the potential is reset to some lower level. The first passage time of the Wiener process is known to obey the inverse gaussian distribution,

$$p(T) = \left(\frac{b}{2\pi T^3} \right)^{1/2} \exp \left(-\frac{b(T-a)^2}{2a^2 T} \right).$$

The points (CV, SK) for the inverse-gaussian distribution lie on the line $\text{SK} = 3\text{CV}$.

Points and lines derived from these typical distributions are depicted in Figure 3a. We can easily observe from the comparison of Figure 3a and Figure 2 that these simple models do not account for the biological data, which are widely distributed in the plane. We are thus motivated to consider a more realistic model.

4 Leaky Integrate-and-Fire Model and the Ornstein-Uhlenbeck Process

A neuron is most simply modeled as an integrator of incoming spike signals. A spike signal arriving at a synaptic junction adds an increment or a decrement to the membrane potential of a neuron. If the cell membrane potential exceeds a certain threshold value, a neuron fires and emits a spike, and then the potential quickly returns to a near-resting level. Another important characteristic of the electrical process is that the membrane potential of a neuron tends to decay toward the resting level in a certain time scale (see, for instance, Nicholls, Martin, & Wallace, 1992).

There are many mathematical models for the membrane dynamics (see, for instance, Tuckwell, 1988). The leaky integrate-and-fire model is the simplest one of these that captures the essential ingredients of the membrane dynamics. This model can be written as

$$\frac{du}{dt} = -\frac{u}{\tau} + (\text{inputs}),$$
$$\text{if } u > u_1, \text{ then } u \rightarrow u_0,$$

where u represents the membrane potential of the cell body measured from its resting level, and τ is the membrane time constant. The original inputs are delta functions of time, which represent (positive) excitatory postsynaptic potentials (EPSPs) and (negative) inhibitory postsynaptic potentials (IPSPs). If the individual inputs are sufficiently small in magnitude compared to the height of the threshold value, and if the events are temporally independent, then the inputs can be treated as constituting the delta-correlated stationary stochastic process,

$$(\text{inputs}) = (\text{mean}) + (\text{fluctuation}).$$

In addition, if the "fluctuation" term represents gaussian white noise, then the dynamics are identical to the Ornstein-Uhlenbeck process (OUP),
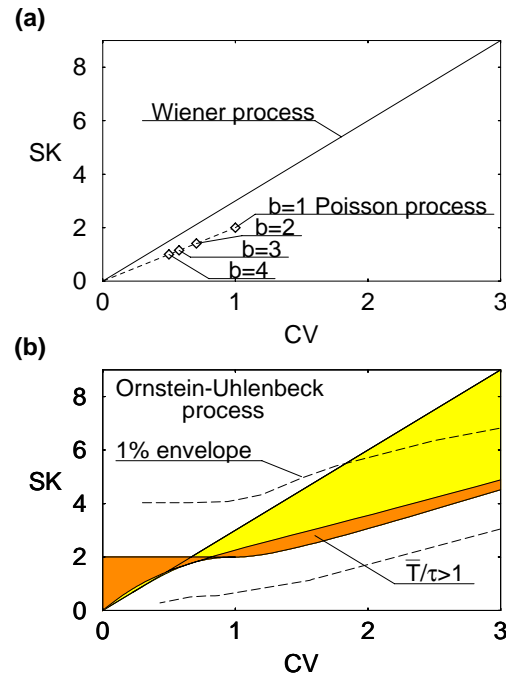
Figure 3: (a) Points and lines in the CV-SK plane derived from several typical model processes. Accumulated Poisson processes for which the number of excitation inputs are $b = 1$ (the Poisson process) and $b = 2, 3, 4, \cdots$ lie on the line $SK = 2CV$. The Wiener process can produce a range of CV and SK values. The corresponding points (CV, SK) lie on the line $SK = 3CV$. (b) The OUP feasible region is represented by the shaded areas. We neglect the lightly shaded area, however, because it corresponds to the obviously unacceptable situation $\overline{T}/\tau < 1$. The dashed lines represent the envelope of 1% contours of distribution of (CV, SK) points, each estimated from 100 ISIs obtained in OUP simulations with various parameter choices within the constraint of $\overline{T}/\tau \geq 1$.

and the ISI corresponds to the first passage time starting from u_0 and reaching u_1. Using a suitable transformation, one can reduce the original model to a "normalized" OUP,

$$\frac{dx}{dt} = -x + \xi(t),$$

$$\text{if } x > \omega, \text{ then } x \to \alpha,$$

where ξ is gaussian white noise with ensemble average characteristics $\langle \xi(t) \rangle$

$= 0$ and $\langle \xi(t)\xi(t') \rangle = \delta(t - t')$. This normalized OUP has two independent parameters, α and ω.

There have been a number of studies on the first passage time of the OUP. Although the first passage time density is not known in a closed form, all moments of the first passage time are known in the form of several kinds of series expansions. We summed the first 100 terms of a series expansion formula due to Ricciardi and Sato (1988). We also summed the first 10 terms of an asymptotic expansion formula due to Keilson and Ross (1975). In the appendix, we summarize these two expansion formulas, and show our method of connecting these functions, for the practical estimate of moments.

5 Statistical Examination of the Points (CV, SK)

The OUP exhibits a range of both CV values and SK values. The model, however, does not cover the whole CV-SK plane, even when sweeping through all the possible parameter values. The feasible region in the CV-SK plane is found to be rather localized, as depicted in Figure 3b (shaded region). If we were able to obtain a spike sequence of infinite length and if the corresponding (CV, SK) points were found to lie outside this feasible region, then we could reject the OUP.

Practical experiment, however, does not provide us with spike sequences of infinite length, and we must draw conclusions from data with a finite number of ISIs. We studied spike sequences consisting of 100 ISIs prepared according to methods L1 and L2, and estimated (CV, SK) values for every such set of ISIs. In order to examine these biological data properly, we must estimate the degree of possible deviation due to finiteness of the number of ISIs. We did this using numerical simulations.

For instance, Figure 4 shows the contour map of the distribution of (CV, SK), each of which is estimated from 100 ISIs generated by the Poisson process. If we assume the spiking process to be a Poisson process, then we should directly compare the physiological data, Figure 2, with this distribution, Figure 4. We can see that the biological data are obviously inconsistent with the Poisson process. In fact, the fraction of the number of biological data lying outside this 10% contour is 63.2% in L1 and 61.4% in L2, the fraction outside the 1% contour is 41.0% in L1 and 35.2% in L2, and the fraction outside the 0.1% contour is 26.7% in L1 and 21.0% in L2.

Because we do not know the correct value of biological neuronal parameters, we must consider all model parameter values in the data examination, excluding obviously unacceptable values. We have excluded the model parameter values that lead to $\overline{T}/\tau < 1$ for the following reason. Among the experimental spike sequences, the mean interspike interval, which corresponds to $\overline{T}$, is at least 30 msec and typically greater than 100 msec. In other words, the average spike rate is fewer than 10 spikes per second. On the other hand, the membrane time constant, which corresponds to τ, is considered to range from 1 to 20 msec (see, for instance, Nicholls, Martin, & Wallace,
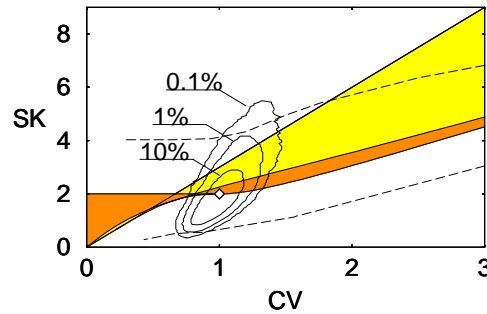
Figure 4: Contour map of the distribution of (CV, SK) values, each estimated from 100 ISIs generated by the Poisson process.

1992; Thomson & Deuchars, 1997). The ratio of the mean spike interval and the membrane time scale $\overline{T}/\tau$ should thus be much greater than unity. The constraint of excluding model parameter values that give $\overline{T}/\tau < 1$ is thus quite reasonable and sufficiently mild. The feasible region so determined ($\overline{T}/\tau \geq 1$) is also depicted in Figure 3b (the heavily shaded region).

For a given parameter set that satisfies the constraint ($\overline{T}/\tau \geq 1$), we numerically obtained a contour map of the probability distribution of (CV, SK) values, each estimated from 100 ISIs generated from Langevin simulations of the OUP. We then moved to a different parameter set to obtain another contour map of the probability distribution, centered at a different position. By repeating this within the region of model parameter values bounded by the above-mentioned constraint, we are able to determine the envelope of 1% contours for the set of all such OUP simulations. This is also depicted in Figure 3b (dashed lines).

The number of experimental data lying outside this envelope of 1% contours is expected to be (much) less than 1% of the total if the OUP (within the reasonable parameter range) is to be considered a good model of neuronal spiking. In Figure 5, we compare this 1% envelope with the biological data obtained using L1 and L2. The number of data lying outside the 1% envelope, however, turned out to be 48 in the case of L1, which represents 7.2% of the 666 spike sequences, and 29 in the case of L2, which represents 4.7% of the 611 spike sequences. Thus, we can reject the pure OUP as a good model of the spiking process based on the results for both methods L1 and L2.

Up to this point we have adopted $\overline{T}/\tau \geq 1$ as a basic constraint for the data examination. This constraint is reasonable in this situation, because the membrane time constant τ is considered to be at most 20 msec, and the
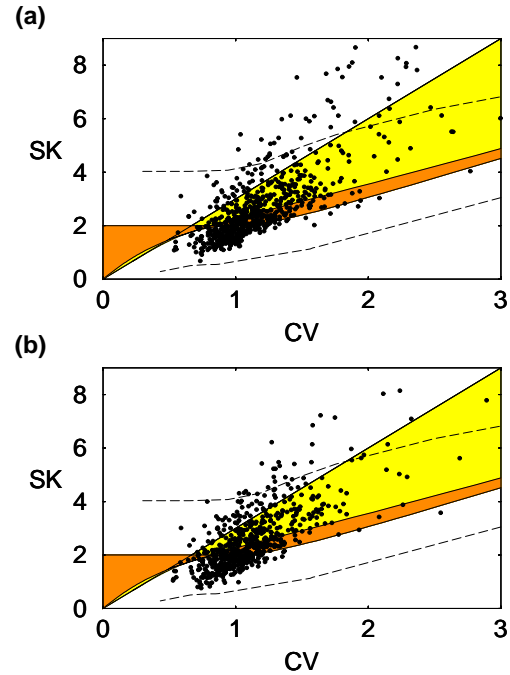
(a)

(b)

Figure 5: Comparison of the biological data with the envelope of 1% contours obtained in OUP simulations with various parameter choices (dashed line). Plots (a) and (b) represent the data corresponding to L1 and L2, respectively. The fraction of the data lying outside the envelope turned out to be 7.2% for L1 and 4.7% for L2.

mean interspike interval $\overline{T}$ in our data is at least 30 msec. In a typical case, we have $\overline{T}/\tau \sim 10$, because τ is typically 10 msec and $\overline{T}$ is typically 100 msec.

It would be interesting, however, to examine the case of smaller $\overline{T}/\tau$. This happens if some slower processes are taking place in a neuron, and the decay time constant τ is larger than the mean interspike interval $\overline{T}$. Let us consider the looser condition, $\overline{T}/\tau \geq 0.1$, which means that the decay time constant τ can be as much as 300 msec, regarding the present data. We can determine the new 1% envelope for this excessively loose condition and enumerate the number of data lying outside the 1% envelope. The number of data lying outside the new 1% envelope turned out to be 27 in L1 (4.1% of 666) and 10 in L2 (1.6% of 611), and we can still reject this excessively loose constraint $\overline{T}/\tau \geq 0.1$. Furthermore, let us examine the loosest condition: no constraint on the time constant. We can also determine the 1% envelope for this no-constraint case. The number of data lying outside the new 1%

envelope is 13 in L 1 (2.0% of 666) and 3 in L2 (0.5% of 611). We should point out that this no constraint on the time constant τ, as well as the excessively loose constraint $\overline{T}/\tau \geq 0.1$, is not biologically reasonable.

The data lying outside the original 1% envelope (dashed lines) generally have large SK values (see Figure 5). It is important to note that the fraction of the number of such data is smaller in the L2 case (4.7%) than in the L1 case (7.2%). We saw in section 2 that L2 has a tendency to neglect long intervals, comparable in length to that of the individual segment interval. The major cause of the large SK values is thus the presence of a few anomalous long intervals embedded in a spike sequence.

6 Discussion

In a heated discussion aroused by Softky and Koch (1993), most studies have been focused on the irregularity of the spike sequence, or a large CV value. As Shadlen and Newsome (1994) pointed out, the simple leaky integrate-and-fire model can reproduce the observed spiking irregularity if the inhibition is balanced with the excitation. This is also true of the OUP, which is naturally derived from the leaky integration assumption. In this article, we proposed examining spiking data on the basis of the coefficient of variation, CV, and the skewness coefficient, SK. We have analyzed the spiking data recorded from the prefrontal cortex of rhesus monkeys on the plane determined by these two coefficients. As a result, the data are found to be inconsistent with the genuine Ornstein-Uhlenbeck process if the model time constant is chosen within the reasonable range.

The inconsistency is mainly due to the data of large SK values. The anomalous long intervals embedded in spike sequences could be a cause of this discrepancy. There is a possibility that the anomalous long intervals are due to experimental error. This could result, for instance, if the relative distance between a microelectrode and a neuron gradually changed and a spike discriminator thus failed to detect actual spikes for a period. Thus, a more detailed examination of the original spike sequence is desirable. However, the result obtained from spike sequences prepared by the method L2, which has the tendency to remove quite long intervals, still rejects the genuine OUP. This implies that the disagreement cannot be due simply to experimental error. It represents a real inconsistency.

We must keep in mind that there is an additional possibility for error to enter in the data preparation, owing to the principle of linkage itself. We linked spike sequences of different trials, assuming that each neuron is statistically subject to the same conditions when under the influence of the same cue stimulus. This is true if the neuronal assembly always assumes a definite stationary state (in a statistical sense) that depends only on the cue stimulus. Monkey's unsuccessful trials are interpreted here as failures of neuronal assembly in maintaining a particular stationary state, and thus we removed all the data from unsuccessful trials. There is, of course, a

possibility that the apparent stationary state existing in the delay period is not uniquely determined by the cue stimulus alone, but that it also reflects various other factors. If we were able to obtain truly long stationary spike sequences, we would not be bothered with these complicated linkage procedures, and we could directly compare the data on the basis of the (CV, SK). We should note, however, that it is not easy to prove that any given neuron is in a statistically stationary condition for a long period. Active animals are generally not stationary, and therefore the neuronal spiking cannot be stationary either if the neurons are more or less involved in the animal's behavior. The present highly controlled delay-response task succeeded in maintaining the monkey's temporally stationary state during this delay period. Thus, we believe that the present data are of relatively good quality as biological data.

If we can assume that the data are free from possible experimental errors, then we should revise our understanding of fundamental and environmental conditions of neuronal spiking. In this case, we must reexamine the three fundamental assumptions used in deriving the Ornstein-Uhlenbeck process: those concerning the linear integration mechanism, the decay of the membrane potential, and the delta-correlated stationarity of incoming inputs to a neuron. A plausible mechanism that could be added to the original integration mechanism is a nonlinear shunting inhibition, in which the inhibition current is strong enough suddenly to cancel the membrane potential accumulated to that point. If the shunting inhibition is brought about by some other simple Poisson process, however, a neuron would be subject to a random interruption, which would bring about a relatively short silence. Thus, the nonlinear shunting mechanism of this kind does not appear to explain the anomalous long intervals. It appears that we rather have to start with a thorough examination of all sorts of statistical structure of the incoming inputs to a neuron.

Appendix

We summarize here the method we used to obtain the first-, second-, and third-order cumulants of the first passage time T of the OUP. These cumulants respectively correspond to

$$C_1 = \overline{T}, \quad C_2 = \overline{(T - \overline{T})^2}, \quad C_3 = \overline{(T - \overline{T})^3}.$$

Each cumulant C_k, which is a function of the initial position α and the threshold ω, can be decomposed as $C_k(\alpha, \omega) = \psi_k(\alpha) - \psi_k(\omega)$. Each ψ_k is given by the set of other functions $\{\phi_k\}_k$ as

$$\psi_1 = \phi_1, \quad \psi_2 = \phi_2 - \phi_1^2, \quad \psi_3 = \phi_3 - 3\phi_2\phi_1 + 2\phi_1^3.$$

The functions $\{\phi_k(x)\}_k$ are not known in a closed form, but are known in the form of several kinds of series expansions. A series expansion formula

due to Ricciardi and Sato (1988) is

$$\phi_1^{RS}(x) = \sum_{n=1}^{L} \gamma(n)x^n,$$

$$\phi_2^{RS}(x) = 2\sum_{n=1}^{L} \gamma(n)\omega_1(n)x^n,$$

$$\phi_3^{RS}(x) = 3\sum_{n=1}^{L} \gamma(n)(\omega_2(n) + \omega_1^2(n))x^n,$$

where,

$$\gamma(1) = -\sqrt{\frac{\pi}{2}}, \quad \gamma(2) = -\frac{1}{2},$$

$$\gamma(n+2) = \frac{n}{(n+2)(n+1)}\gamma(n), \quad (n \geq 1),$$

$$\omega_k(0) = 0, \quad \left\{ \begin{array}{ccc} \omega_1(1) & = & \ln 2 \\ \omega_2(1) & = & \dfrac{\pi^2}{12} \end{array} \right. , \quad \omega_k(n+2) = \omega_k(n) - \frac{1}{n^k}.$$

An asymptotic formula due to Keilson and Ross (1975) is

$$\phi_1^{KR}(x) = \sum_{n=0}^{M} x^{-2n}(p_n^{(0)}\ln|x| + p_n^{(1)}),$$

$$\phi_2^{KR}(x) = 2\sum_{n=0}^{M} x^{-2n}\left(\frac{1}{2}p_n^{(0)}\ln^2|x| + p_n^{(1)}\ln|x| + p_n^{(2)}\right),$$

$$\phi_3^{KR}(x) = 3!\sum_{n=0}^{M} x^{-2n}\left(\frac{1}{3!}p_n^{(0)}\ln^3|x| + \frac{1}{2}p_n^{(1)}\ln^2|x| + p_n^{(2)}\ln|x| + p_n^{(3)}\right),$$

where,

$$\left(\begin{array}{c} p_0^{(0)} \\ p_0^{(1)} \\ p_0^{(2)} \\ p_0^{(3)} \end{array} \right) = \left(\begin{array}{c} 1 \\ 0.63518142 \\ 0.81857797 \\ 0.78512305 \end{array} \right),$$

$$\left(\begin{array}{c} p_{n+1}^{(0)} \\ p_{n+1}^{(1)} \\ p_{n+1}^{(2)} \\ p_{n+1}^{(3)} \end{array} \right) = \left(\begin{array}{cccc} a_n & & & 0 \\ b_n & a_n & & \\ c_n & b_n & a_n & \\ 0 & c_n & b_n & a_n \end{array} \right) \left(\begin{array}{c} p_n^{(0)} \\ p_n^{(1)} \\ p_n^{(2)} \\ p_n^{(3)} \end{array} \right),$$

$$a_n \equiv -\frac{2n(2n+1)}{2n+2}, \quad b_n \equiv \frac{2n+(2n+1)}{2n+2}, \quad c_n \equiv -\frac{1}{2n+2}.$$

For the practical estimate of the cumulants, we summed the first 100 terms for the RS expansion formula ($L = 100$) and the first 10 terms for the KR expansion formula ($M = 10$). In order to connect these functions sufficiently smoothly, we sought the best position to switch these expansion formulas, respectively, for each ϕ_k,

$$
\begin{array}{llll}
\phi_1^{KR}(x) & \text{for} \quad x < -5.70, & \phi_1^{RS}(x) & \text{for} \quad -5.70 \leq x, \\
\phi_2^{KR}(x) & \text{for} \quad x < -5.55, & \phi_2^{RS}(x) & \text{for} \quad -5.55 \leq x, \\
\phi_3^{KR}(x) & \text{for} \quad x < -5.50, & \phi_3^{RS}(x) & \text{for} \quad -5.50 \leq x.
\end{array}
$$

By means of these expansion formulas, we estimated the CV and SK values,

$$\text{CV} = \frac{C_2^{1/2}}{C_1}, \quad \text{SK} = \frac{C_3}{C_2^{3/2}}.$$

Acknowledgments

References

Abeles, M. (1991). *Corticonics—Neural circuits of the cerebral cortex*. Cambridge: Cambridge University Press.

Amit, D. J., & Brunel, N. (1997). Global spontaneous activity and local structured (learned) delay activity in cortex. *Cerebral Cortex, 7*, 237–252.

Funahashi, S., Bruce, C. J., & Goldman-Rakic, P. S. (1989). Mnemonic coding of visual space in the monkey's dorsolateral prefrontal cortex. *J. Neurophysiology, 61*, 331–349.

Funahashi, S., & Inoue, M. (1999). Neuronal interactions related to working memory processes in the primate prefrontal cortex revealed by cross-correlation analysis. Work in preparation. Kyoto: Kyoto University.

Gerstein, G. L., & Mandelbrot, B. (1964). Random walk models for the spike activity of a single neuron. *Biophys. J., 4*, 41–68.

Goldman-Rakic, P. S., Bruce, D. C. J., & Funahashi, S. (1990). Neocortical memory circuits. In *Cold Spring Harbor Symposia on Quantitative Biology* (vol. 55, pp. 1025–1038). Cold Spring Harbor, NY: Cold Spring Harbor Laboratory Press.

Inoue, J., & Sato, S. (1993). Pearson plot of the first-passage-time distribution of the Ornstein-Uhlenbeck process and fitting of the distribution to the normal firing interval histogram. *Transactions of the Institute of Electronics, Information and Communication Engineers* (Japan), *J76-A*, 1011–1017.

Inoue, J., Sato, S., & Ricciardi, L. M. (1995). On the parameter estimation for diffusion models of a single neuron's activities. *Biol. Cybern., 73*, 209–221.

Ishizuka, N., Cowan, W. M., & Amaral, D. G. (1995). A quantitative analysis of the dendritic organization of pyramidal cells in the rat hippocampus. *J. Comparative Neurology, 362*, 17–45.

Keilson, J., & Ross, H. F. (1975). Passage time distribution for gaussian Markov (Ornstein-Uhlenbeck) statistical processes. *Selected Tables in Mathematical Statistics, 3*, 233–327.

Lánský, P., & Radil, T. (1987). Statistical inference on spontaneous neuronal discharge patterns. *Biol. Cybern., 55*, 299–311.

Nicholls, J. G., Martin, A. R., & Wallace, B. G. (1992). *From neuron to brain* (3rd ed.). Sunderland, MA: Sinauer.

Ricciardi, L. M., & Sato, S. (1988). First-passage-time density and moments of the Ornstein-Uhlenbeck process. *J. Appl. Prob., 25*, 43–57.

Shadlen, M. N., & Newsome, W. T. (1994). Noise, neural codes and cortical organization. *Current Opinion in Neurobiology, 4*, 569–579.

Shinomoto, S., & Sakai, Y. (1998). Spiking mechanisms of cortical neurons. *Philosophical Magazine, 77*, 1549–1555.

Softky, W. R., & Koch, C. (1993). The highly irregular firing of cortical cells is inconsistent with temporal integration of random EPSPs. *J. Neuroscience, 13*, 334–350.

Thomson, A. M., & Deuchars, J. (1997). Synaptic interactions in neocortical local circuits: Dual intracellular recordings in vitro. *Cerebral Cortex, 7*, 510–522.

Tsodyks, M. V., & Sejnowski, T. (1995). Rapid state switching in balanced cortical network models. *Network, 6*, 111–124.

Tuckwell, H. C. (1988). *Introduction to theoretical neurobiology*, Cambridge: Cambridge University Press.

van Vreeswijk, C., & Sompolinsky, H. (1996). Chaos in neural networks with balanced excitatory and inhibitory activity. *Science, 274*, 1724–1726.

This article has been cited by:

2. Umberto Picchini, Susanne Ditlevsen, Andrea De Gaetano, Petr Lansky. 2008. Parameters of the Diffusion Leaky Integrate-and-Fire Neuronal Model for a Slowly Fluctuating Signal. *Neural Computation* **20**:11, 2696-2714. [Abstract] [PDF] [PDF Plus]

3. Kukjin Kang, Shun-ichi Amari. 2008. Discrimination with Spike Times and ISI Distributions. *Neural Computation* **20**:6, 1411-1426. [Abstract] [PDF] [PDF Plus]

4. Alfonso Renart, Rubén Moreno-Bote, Xiao-Jing Wang, Néstor Parga. 2007. Mean-Driven and Fluctuation-Driven Persistent Activity in Recurrent Networks. *Neural Computation* **19**:1, 1-46. [Abstract] [PDF] [PDF Plus]

5. Hiroyuki Nakahara , Shun-ichi Amari , Barry J. Richmond . 2006. A Comparison of Descriptive Models of a Single Spike Train by Information-Geometric Measure. *Neural Computation* **18**:3, 545-568. [Abstract] [PDF] [PDF Plus]

6. Kazushi Ikeda . 2005. Information Geometry of Interspike Intervals in Spiking Neurons. *Neural Computation* **17**:12, 2719-2735. [Abstract] [PDF] [PDF Plus]

7. B. Scott Jackson . 2004. Including Long-Range Dependence in Integrate-and-Fire Models of the High Interspike-Interval Variability of Cortical Neurons. *Neural Computation* **16**:10, 2125-2195. [Abstract] [PDF] [PDF Plus]

8. Shigeru Shinomoto , Keisetsu Shima , Jun Tanji . 2003. Differences in Spiking Patterns Among Cortical Neurons. *Neural Computation* **15**:12, 2823-2842. [Abstract] [PDF] [PDF Plus]

9. Emilio Salinas , Terrence J. Sejnowski . 2002. Integrate-and-Fire Neurons Driven by Correlated Stochastic Input. *Neural Computation* **14**:9, 2111-2155. [Abstract] [PDF] [PDF Plus]